

**Surface Reconstruction by
Coupled Depth/Slope Model with
Natural Boundary Conditions**

by
Ying Li

Technical Report 91-24
November 1991

Department of Computer Science
University of British Columbia
Rm 333 - 6356 Agricultural Road
Vancouver, B.C.
CANADA V6T 1Z2

Surface Reconstruction by Coupled Depth/Slope Model with Natural Boundary Conditions

by
Ying Li

Department of Computer Science
The University of British Columbia
Vancouver, B. C. V6T 1Z2
Canada

email: li@cs.ubc.ca

Abstract

This paper reports on an IRIS project of reconstructing surface height from gradient. The coupled depth/slope model developed by J. G. Harris has been used and augmented with natural boundary conditions. Experiments have been conducted with emphasis on how to deal with uncertainties about boundary values. Experiments have shown that the reconstructed surfaces are confined to the original shapes if accurate boundary values are given. The algorithm fails to produce correct shapes when inaccurate boundary values are used. Natural boundary conditions are necessary conditions for the problem of variational calculus to be solved. Experiments have shown that natural boundary conditions can be relied upon when no estimations of boundary values can be made, except on occluding boundaries. When relative boundary values of occluding boundaries can be assumed, good reconstruction results can be obtained.

1 Introduction

This paper reports on an IRIS project of reconstructing surface height from gradient. The coupled depth/slope model developed by Harris [2] has been used and augmented with natural boundary conditions. Experiments have been conducted with emphasis on how to deal with uncertainties about boundary values.

Section 2 reviews the coupled depth/slope model. Section 3 develops the natural boundary conditions for the coupled depth/slope model. Section 4 develops an iterating scheme and an algorithm based on both the coupled depth/slope model and the natural boundary conditions. Section 5 describes the design of various experiments on the algorithm and analyze the experimental results.

Throughout this paper z denotes surface height, $z = z(x, y)$, and (p, q) denotes surface gradient. The gradients of surfaces are obtained by the photometric stereo method of Woodham [6]. The plane of the paper denotes the xy plane with x axis pointing to the left and y axis pointing downwards, and z axis pointing to us perpendicular to the xy pane.

2 The Coupled Depth/Slope Model

The problem that Harris [2] addresses is to reconstruct a surface from sparse sensory data. Harris built his coupled depth/slope model as a network of ideal subtractor elements connected by two planes of resistor meshes. The power dissipated in the total network is found to be

$$\begin{aligned} E &= \iint [(z_x - p)^2 + (z_y - q)^2 + p_x^2 + p_y^2 + q_x^2 + q_y^2] dx dy \\ &= \iint F(x, y, z, z_x, z_y, p, p_x, p_y, q, q_x, q_y) dx dy \end{aligned} \quad (1)$$

Maxwell's minimum heat theorem states that the distribution of currents and voltages in a circuit is such that the total power dissipated as heat is minimized. Thus the problem becomes a problem of the calculus of variations.

The Euler-Lagrange equations for (1) are (see Courant-Hilbert [1] page 192)

$$\begin{aligned} -[F]_z &\triangleq \frac{\partial}{\partial x} F_{z_x} + \frac{\partial}{\partial y} F_{z_y} - F_z = 0, \\ -[F]_p &\triangleq \frac{\partial}{\partial x} F_{p_x} + \frac{\partial}{\partial y} F_{p_y} - F_p = 0, \\ -[F]_q &\triangleq \frac{\partial}{\partial x} F_{q_x} + \frac{\partial}{\partial y} F_{q_y} - F_q = 0. \end{aligned}$$

Calculating F_z , F_{z_x} , and F_{z_y} , we have

$$F_z = 0, F_{z_x} = 2(z_x - p), F_{z_y} = 2(z_y - q).$$

Substituting them into $[F]_z$, we get a differential equation

$$\Delta z = p_x + q_y.$$

Similar substitutions in $[F]_p$ and $[F]_q$ result in the following equations

$$\Delta p = -(z_x - p), \Delta q = -(z_y - q).$$

Thus Harris got his *system of coupled differential equations*

$$\Delta z = p_x + q_y, \tag{2}$$

$$\Delta p = p - z_x, \tag{3}$$

$$\Delta q = q - z_y. \tag{4}$$

3 Natural Boundary Conditions

The functions to be determined by the differential equations in the previous section are postulated to assume prescribed values at the boundary of the region of integration. If no boundary conditions are prescribed for the unknown functions in a fixed basic region, we speak of free boundary values. *Natural boundary conditions* for free boundaries are necessary conditions, in

addition to the Euler equations, for the variation to vanish. The natural boundary conditions for (1) are (see Courant-Hilbert [1] page 209)

$$F_{z_x} \frac{dy}{ds} - F_{z_y} \frac{dx}{ds} = 0 ,$$

$$F_{p_x} \frac{dy}{ds} - F_{p_y} \frac{dx}{ds} = 0 ,$$

$$F_{q_x} \frac{dy}{ds} - F_{q_y} \frac{dx}{ds} = 0 ,$$

on the boundary of the region whose arc length is denoted by s . Calculating F_{z_x} , F_{z_y} , and so on, we have

$$\begin{aligned} (z_x - p) \frac{dy}{ds} - (z_y - q) \frac{dx}{ds} &= 0 , \\ p_x \frac{dy}{ds} - p_y \frac{dx}{ds} &= 0 , \\ q_x \frac{dy}{ds} - q_y \frac{dx}{ds} &= 0 . \end{aligned}$$

Since $(\frac{dy}{ds}, -\frac{dx}{ds})$ is a normal to the boundary, the natural boundary conditions state that *the normal derivative of the gradient is zero and the normal derivative of the height has to match the slope in the normal direction computed from the gradient* (Horn [3] page 29). Let n be a normal direction to the boundary, the natural boundary conditions can be represented as

$$\frac{\partial z}{\partial n} = \langle (p, q), n \rangle , \tag{5}$$

$$\frac{\partial p}{\partial n} = 0 , \tag{6}$$

$$\frac{\partial q}{\partial n} = 0 . \tag{7}$$

4 Iterating Scheme and Algorithm

The xy coordinate system on which our experiments are being conducted is shown in Figure 1, where the relationship between the data array and

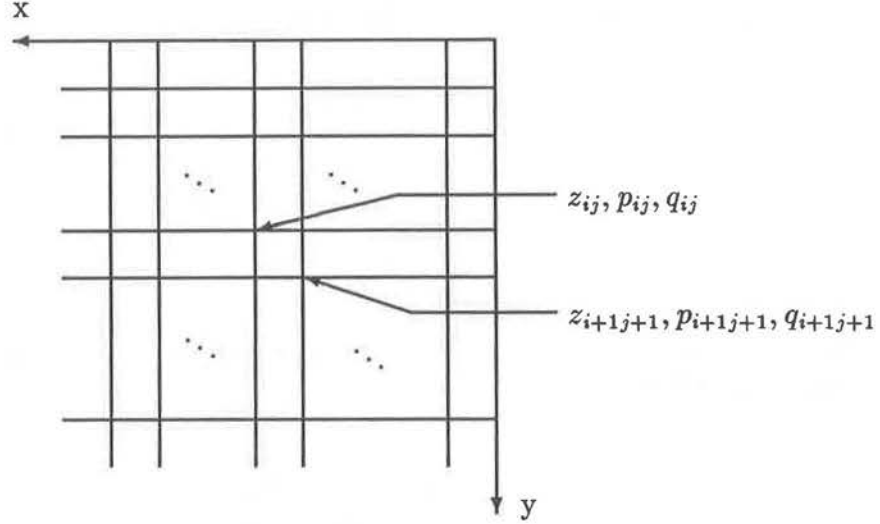


Figure 1: Coordinate system and data array.

the coordinate system is shown. It may look confusing because j increases as x decreases. But it does not affect any part of the theory developed in previous sections. It only affects the appearance of the formula of finite difference approximations of the derivatives. So we only need to remember this relation when we use finite differences.

The finite difference approximations we use for the derivatives in differential equations (2), (3), and (4) are

$$\begin{aligned}
 \Delta z &= z_{i+1j} + z_{i-1j} + z_{ij+1} + z_{ij-1} - 4z_{ij} , \\
 \Delta p &= p_{i+1j} + p_{i-1j} + p_{ij+1} + p_{ij-1} - 4p_{ij} , \\
 \Delta q &= q_{i+1j} + q_{i-1j} + q_{ij+1} + q_{ij-1} - 4q_{ij} , \\
 z_x &= z_{ij-1} - z_{ij} \text{ (forward-difference) ,} \\
 z_y &= z_{i+1j} - z_{ij} \text{ (forward-difference) ,} \\
 p_x &= p_{ij} - p_{ij+1} \text{ (backward-difference) ,} \\
 q_y &= q_{ij} - q_{i-1j} \text{ (backward-difference) .}
 \end{aligned}$$

Substituting them into differential equations (2), (3), and (4) and rearranging

the terms, the following discrete equations are obtained:

$$z_{ij} = \frac{1}{4} (z_{i+1j} + z_{i-1j} + z_{ij+1} + z_{ij-1} + p_{ij+1} + q_{i-1j} - p_{ij} - q_{ij}) \quad (8)$$

$$p_{ij} = \frac{1}{5} (p_{i+1j} + p_{i-1j} + p_{ij+1} + p_{ij-1} + z_{ij-1} - z_{ij}) , \quad (9)$$

$$q_{ij} = \frac{1}{5} (q_{i+1j} + q_{i-1j} + q_{ij+1} + q_{ij-1} + z_{i+1j} - z_{ij}) . \quad (10)$$

A direct application of Jacobi iterative scheme on these equations is proved by Harris not to converge. If we add more stability to the iteration as

$$z_{ij}^{k+1} = \frac{1}{4} (z_{i+1j}^k + z_{i-1j}^k + z_{ij+1}^k + z_{ij-1}^k + p_{ij+1}^k + q_{i-1j}^k - p_{ij}^k - q_{ij}^k) , \quad (11)$$

$$p_{ij}^{k+1} = \frac{1}{5} (p_{i+1j}^k + p_{i-1j}^k + p_{ij+1}^k + p_{ij-1}^k + z_{ij-1}^{k+1} - z_{ij}^{k+1}) , \quad (12)$$

$$q_{ij}^{k+1} = \frac{1}{5} (q_{i+1j}^k + q_{i-1j}^k + q_{ij+1}^k + q_{ij-1}^k + z_{i+1j}^{k+1} - z_{ij}^{k+1}) , \quad (13)$$

the iteration converges.

To get the iterating formula on the boundary using the natural boundary conditions, let (i, j) be a point on the boundary, (ii, jj) be the point inside the region such that the direction from (ii, jj) to (i, j) is closest to the outward normal direction n_{ij} at (i, j) . Then substituting the derivatives in equations (5), (6), and (7) by their finite difference approximations, and rearranging the terms, the following iterating scheme for z , p , and q on the boundary of the region are obtained:

$$z_{ij}^{k+1} = z_{ii jj}^k + \langle (p_{ij}^k, q_{ij}^k), n_{ij} \rangle , \quad (14)$$

$$p_{ij}^{k+1} = p_{ii jj}^k , \quad (15)$$

$$q_{ij}^{k+1} = q_{ii jj}^k . \quad (16)$$

Employing the just mentioned iterating scheme and formula, we have the following algorithm.

Algorithm

1. Input p_{ij}^0 , q_{ij}^0 , and z_{ij}^0 . Let $k = 0$, K be the maximal number of iterations.
2. For each (i, j) , if (i, j) is inside the region, set z_{ij}^{k+1} according to (11); if (i, j) is on the boundary of the region, set z_{ij}^{k+1} according to (14).
3. For each (i, j) , if (i, j) is inside the region, set p_{ij}^{k+1} and q_{ij}^{k+1} according to (12) and (13); if (i, j) is on the boundary of the region, set p_{ij}^{k+1} and q_{ij}^{k+1} according to (15) and (16).
4. If $k > K$, or the difference between z^k and z^{k-1} is small, then output z^k , p^k , and q^k , and quit.
5. Else, let $k = k + 1$, go to step 2.

5 Experimentations

The objects used in our experiments are a set of vases. We are given a mask array, called *s-array*, indicating where the interested region is. We are also given a pair of arrays, *p-array* and *q-array*, holding the gradient of the surface obtained by the photometric stereo method of Woodham [6].

Recall that the coupled depth/slope model was designed for reconstructing surface from sparse data. Here, the gradient we have is dense and accurate, i.e., on almost every grid the gradient is accurate. Thus, we basically don't need to update *p-array* and *q-array*. On the other hand, we know nothing about the surface height z . So we need to dedicate most of our computation on the updating of z , and the focus of our attention is on the boundary conditions. A series of experiments has been conducted to test the algorithm. In the following, we will describe the design of each experiment and analyze the results accordingly.

Experiment 1. Coupled depth/slope model with natural boundary conditions on the whole boundary.

If we know nothing about the boundary values of the surface, there is generally no unique solution to the coupled differential equations (2), (3), and (4). We want to apply the natural boundary conditions on the boundary so that we don't need to estimate the boundary values prior to the computation. Natural boundary conditions require the normal to the boundaries. Thanks to the theory and program of Lowe [4], we can have the normal to the boundary ready as long as we know where the boundary points are. We run the algorithm as described in Section 4 except that we don't update the *p-array* and *q-array* inside the region because we believe they are accurate. Figure 2 and Figure 3 plot the reconstructed surfaces with natural boundary conditions imposed on the whole boundary. The result is not what we would expect. One explanation would be that because the gradients tend to infinity at the side occluding boundaries, the surface heights tend to minus infinity to keep up with the gradients. The following experiments are designed to find out what causes the phenomenon.

Experiment 2. Coupled depth/slope model with boundary values being prescribed over the whole boundary.

To find out why **Experiment 1** fails to reconstruct the expected shape, we want to separate the coupled depth/slope model from the natural boundary conditions. Thus we start the algorithm with *z-array* containing prescribed values on the boundaries, update only *z-array* and only update at the interior point of the region.

Figure 4 and Figure 5 show the plot images of the reconstructed surfaces with the boundary value being zero over the whole boundary. The result is as expected that the surface tends to be smoothed over the boundary, because the algorithm assumes the continuity of the first derivatives.

We know that the surface is a surface of revolution, the *s-array* we have is an estimation of the silhouette. Thus the values of half circles at the top and bottom boundaries are better estimations of the boundary values than zero over the whole boundary. Figure 6 and Figure 7 show the reconstructed surfaces with boundary values being the values of half circles on the top and bottom boundaries and zero on the side boundaries. The result is satisfying

but the method is only applicable to vertical solid of revolutions.

Experiment 3. Coupled depth/slope model with natural boundary conditions on one part of the boundary and prescribed boundary values on the rest of the boundary.

Looking at Figure 2 and Figure 3, it is reasonable to believe that the problem lies on the occluding boundary of the object. We run the algorithm with natural boundary conditions being imposed on the top and bottom boundaries and zero boundary value prescribed on the side boundaries. That is, *z-array* is updated according to the coupled depth/slope model in the interior of the region, updated according to natural boundary conditions on the top and bottom boundaries, and kept zero on the side boundaries. Figure 8 to 11 show the reconstructed surfaces. The results are satisfactory as long as we are able to indicate where we want natural boundary conditions to be imposed and we know the boundary value at the rest of the boundary.

Experiment 4. Checking the sensitivity of natural boundary conditions to boundary directions.

Results of **Experiment 1** also alarm us about the possibility of our algorithm being sensitive to the directions of the normals to the boundaries. This experiment is designed to check this out. Figure 12 shows the reconstruction result on a new region, which is obtained from the original region by cutting, at slope 1, its upper-right corner away. The gradient is the original data. The reconstruction assumes natural boundary conditions on top and bottom boundaries, and assumes boundary value zero on the side boundaries. The result is then transposed before it is plotted to have a better view. Figure 13 shows the result of the same procedure as for Figure 12, except that the cutting slope is one half. For this new region, only the point at one end of the cutting edge has unusual big negative value as its reconstructed height. This is not surprising because the boundary has a normal discontinuity at that point. The reconstructed surfaces look as if the surfaces had been cut after reconstruction. This makes the natural boundary conditions more favorable. We then come back to our original region, and transpose the *s-array*, *p-array*, and *q-array*, and do the reconstruction again. Figure 14 shows the reconstructed surface using the transposed *s-array*, *p-array*, and *q-array*. It looks the same as the surface transposed after reconstruction. The conclusion we draw from this experiment is that the natural boundary conditions are not

sensitive to the directions of the normals to the region boundary.

Experiment 5. Coupled depth/slope model with natural boundary conditions on the whole boundary revisited – avoiding occluding boundaries.

So far we haven't got a result which says that we could apply the natural boundary conditions to the whole boundary without being concerned about any prescribed boundary values. In this experiment, we will throw away some points from the original region, so that in the new region we will not use the gradients that approach infinity because of the concerned points being too close to the occluding boundary. Figure 15 shows the reconstructed surface over a new region with the natural boundary conditions imposed on the whole boundary. The new region is obtained by cutting the original region vertically and throw away the original occluding side boundaries. The reconstructed surface is lifted by an offset before it is being plotted, for the reconstructed surface has height starting from a negative value. The reconstructed surface starts its height from a negative value because the iterations are started with zero height and the natural boundary conditions are imposed at the first iteration. By this experiment, we can say that our implementation of the natural boundary conditions works on the whole boundary of the region.

Experiment 6. Coupled depth/slope model with natural boundary conditions on the whole boundary revisited – checking occluding boundaries during reconstruction.

Results of **Experiment 1** also hint us a way of finding occluding boundary points during reconstruction. That is, when surface height at a boundary point tends to minus infinity during the reconstruction, it can be taken as an occluding boundary point. Some objects involved in our experiments are generalized cones with convex cross-section as defined by Marr [5]. By Theorem 1 in Marr [5], the contour generator of the boundaries of the silhouette regions are planar. That is, the points on the three dimensional surface that generate the silhouette boundary points in the images are planar. Thus, we can assume that the occluding boundary points have the same height because we are viewing the surface orthogonally. The procedure of **Experiment 1** is adjusted as follows. All boundary points are dynamic when the procedure is started. At the end of each iteration, check every dynamic boundary point whether its surface height is smaller than a negative threshold. If yes, set

its height to zero, set the point to be non-dynamic and its height remain unchanged throughout the rest of the computation. Figure 16 and Figure 17 show the plot images of the reconstructed surfaces. The result is satisfying. The method is restricted to generalized cones with convex cross-section viewed orthogonally.

6 Conclusion

A surface reconstruction algorithm based on the coupled depth/slope model of Harris has been implemented. The natural boundary conditions for the coupled depth/slope model has been developed and implemented to augment the algorithm. A series of experiments has been conducted, focusing on the effect of the boundary conditions.

The reconstructed surfaces are confined to the original shapes if accurate boundary values are given. The algorithm fails to produce correct shapes when inaccurate boundary values are used. Natural boundary conditions can be relied upon when no estimations of boundary values can be made, except on occluding boundaries. When relative boundary values of occluding boundaries can be assumed, good reconstruction results can be obtained.

The experiments have shown that the implementation of the coupled depth/slope model and the implementation of the developed natural boundary conditions work as expected by theory and intuition.

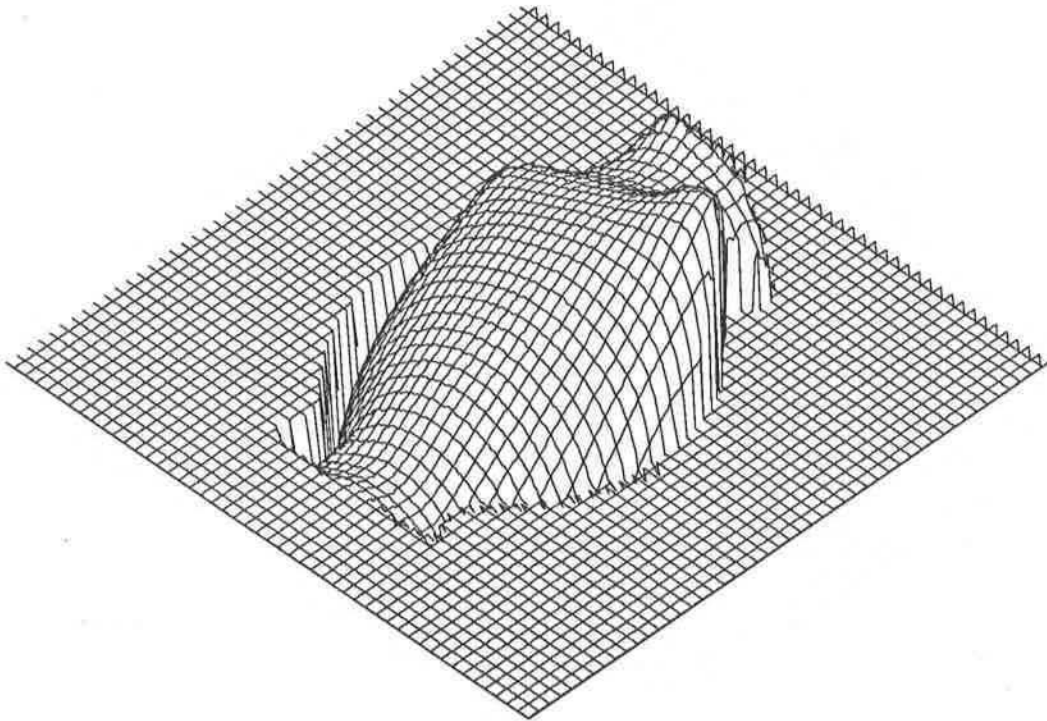


Figure 2: Result of **Experiment 1** – Coupled depth/slope model with natural boundary conditions imposed on the whole boundary.

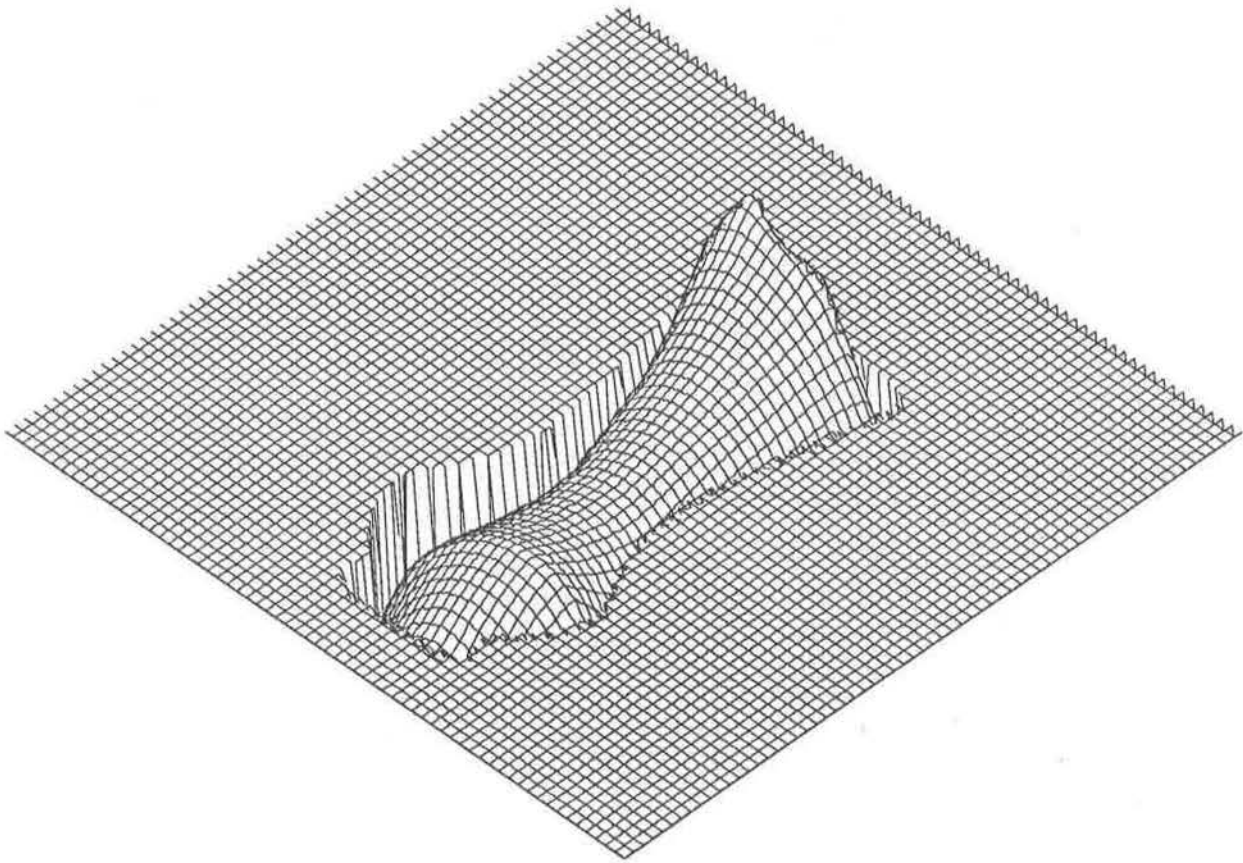


Figure 3: Result of **Experiment 1** – Coupled depth/slope model with natural boundary conditions imposed on the whole boundary.

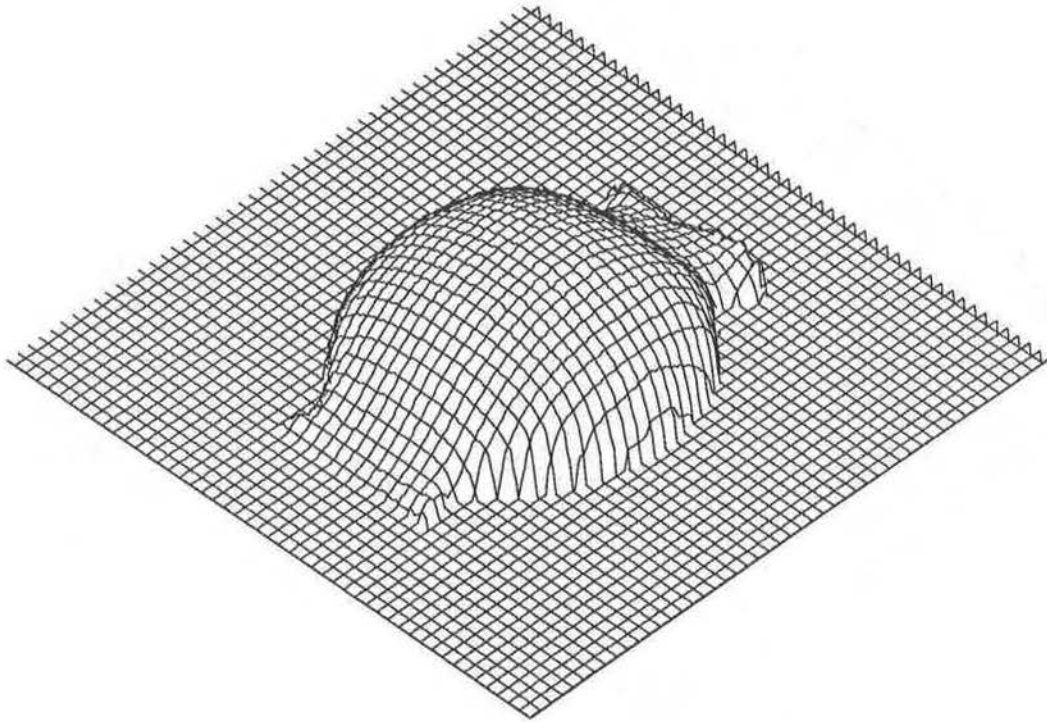


Figure 4: Result of **Experiment 2** – Coupled depth/slope model with prescribed boundary values being zero over the whole boundary.

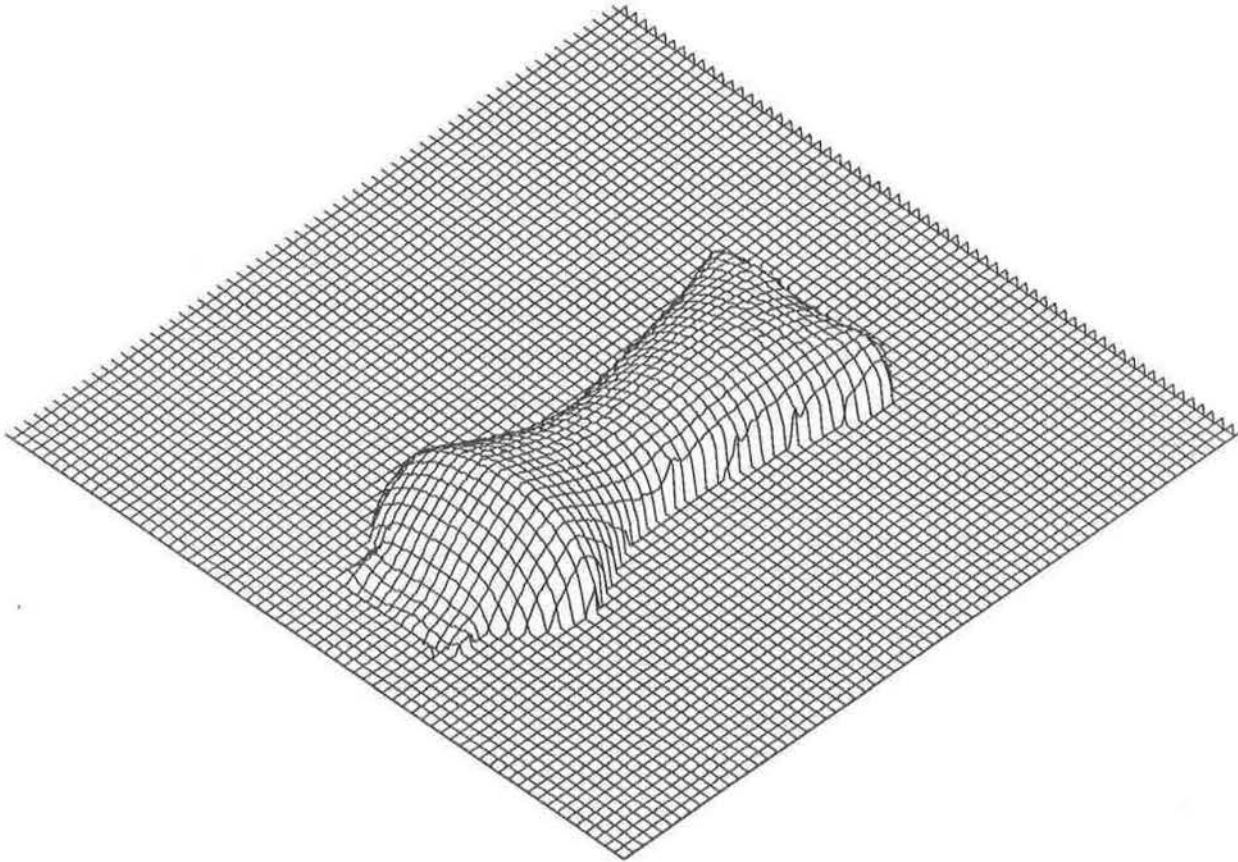


Figure 5: Result of **Experiment 2** – Coupled depth/slope model with prescribed boundary values being zero over the whole boundary.

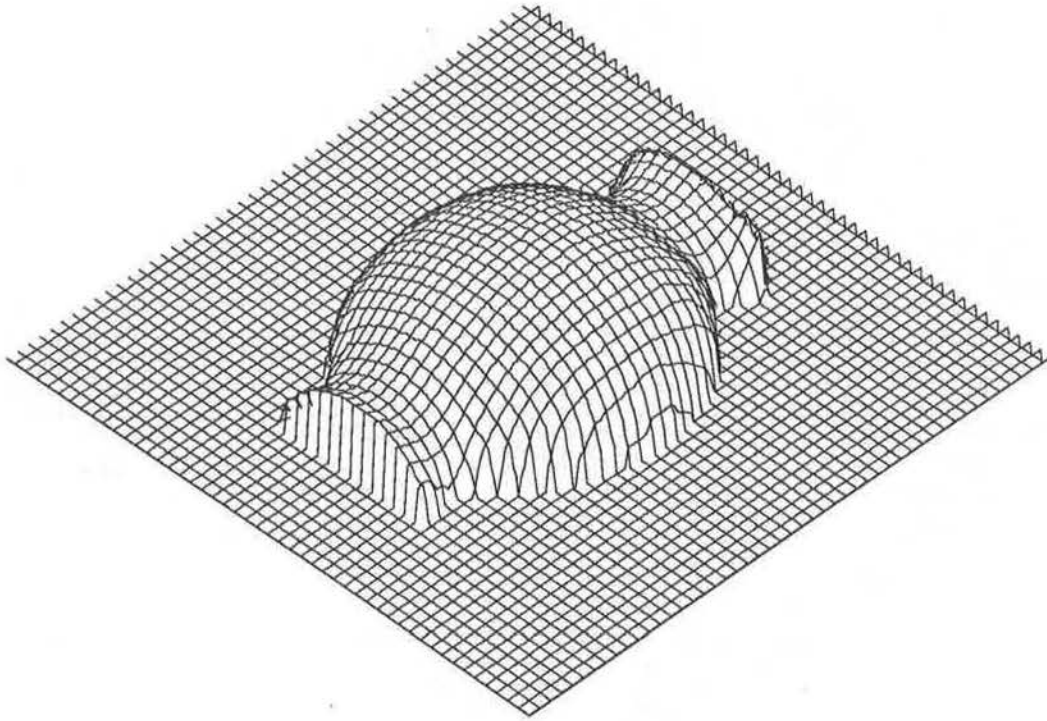


Figure 6: Result of **Experiment 2** – Coupled depth/slope model with prescribed boundary values being zero on the side boundaries and the value of half circles on the top and bottom boundaries.

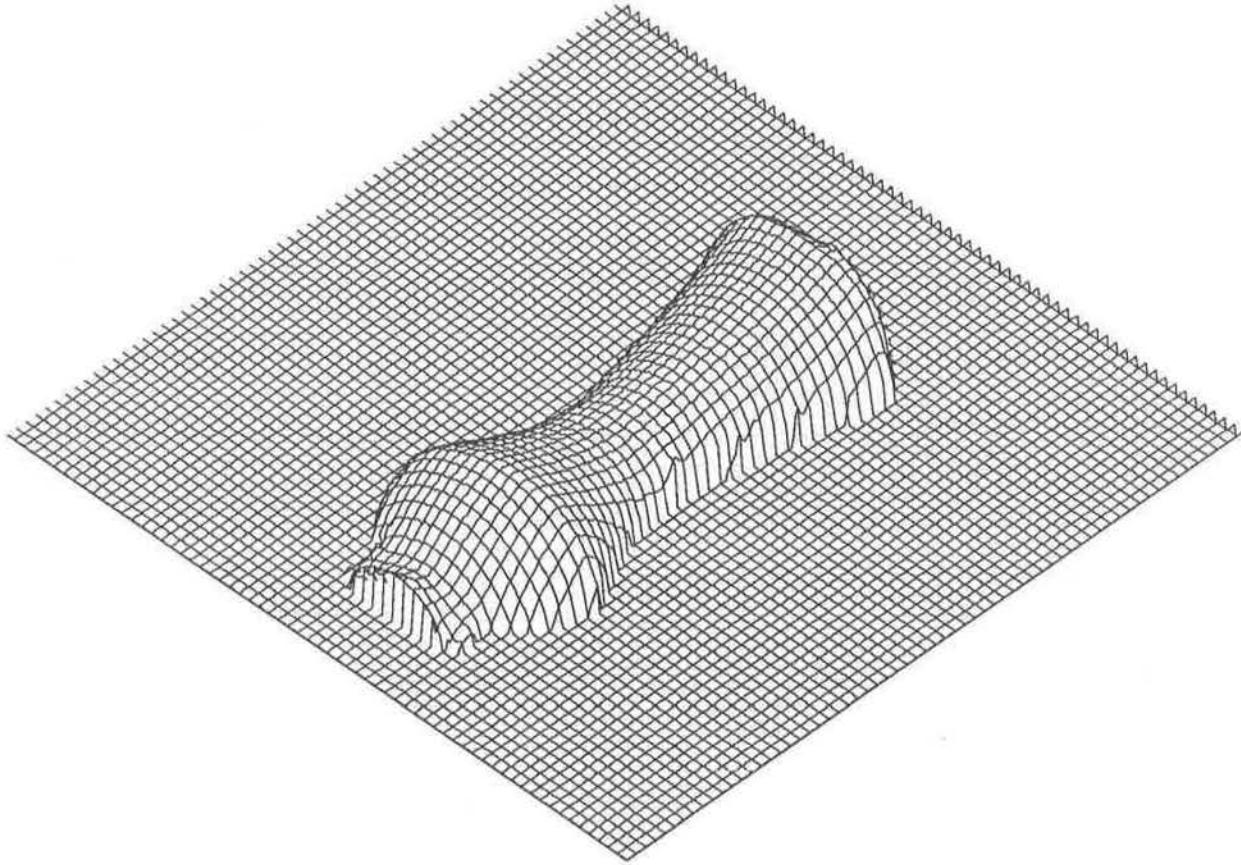


Figure 7: Result of **Experiment 2** – Coupled depth/slope model with prescribed boundary values being zero on the side boundaries and the value of half circles on the top and bottom boundaries.

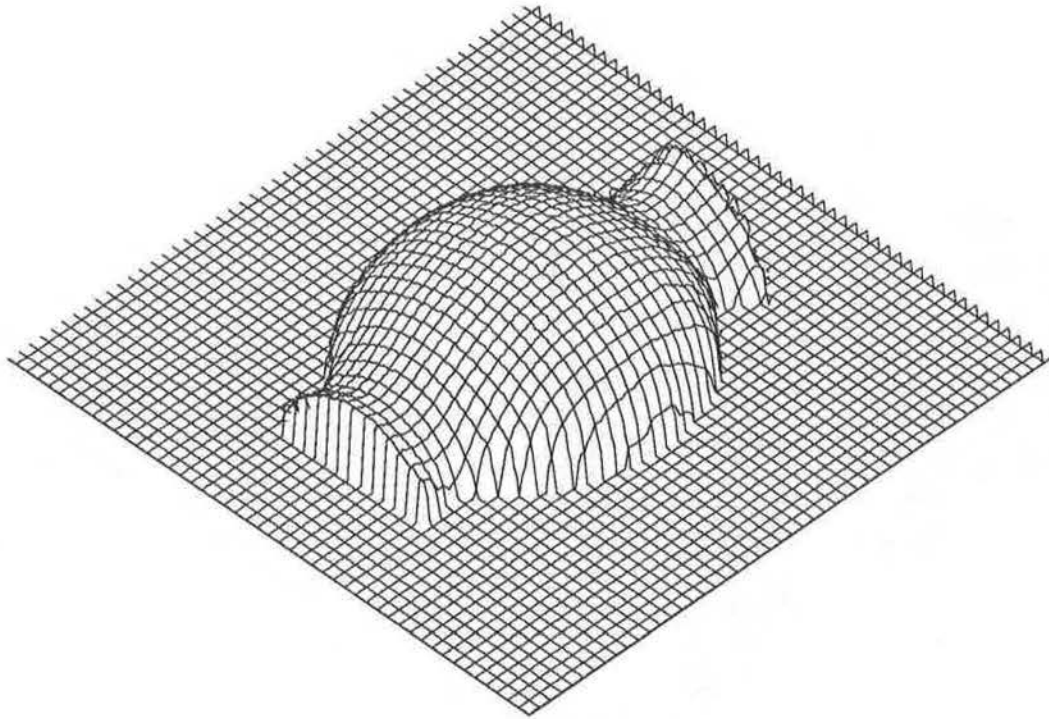


Figure 8: Result of **Experiment 3** – Coupled depth/slope model with prescribed boundary values being zero on the side boundaries and natural boundary conditions being imposed on the top and bottom boundaries.

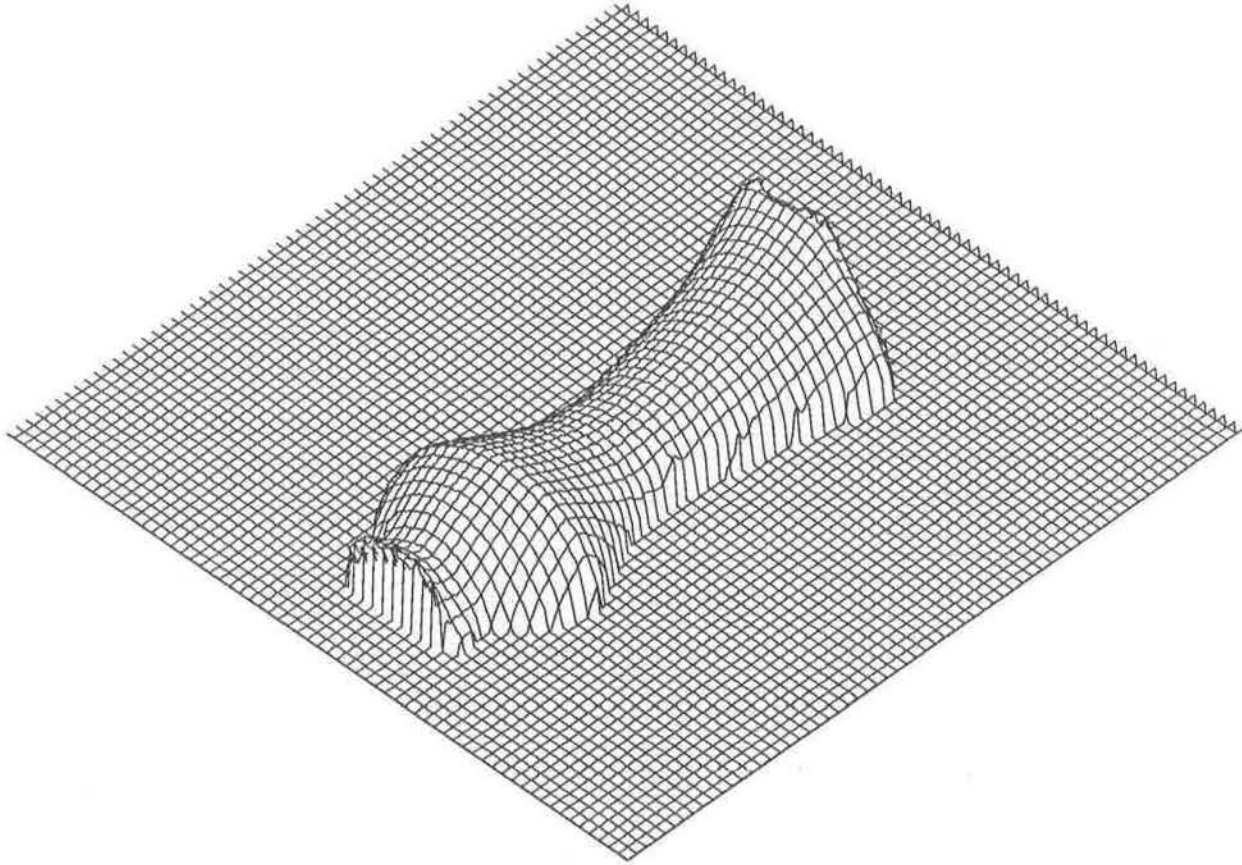


Figure 9: Result of **Experiment 3** – Coupled depth/slope model with prescribed boundary values being zero on the side boundaries and natural boundary conditions being imposed on the top and bottom boundaries.

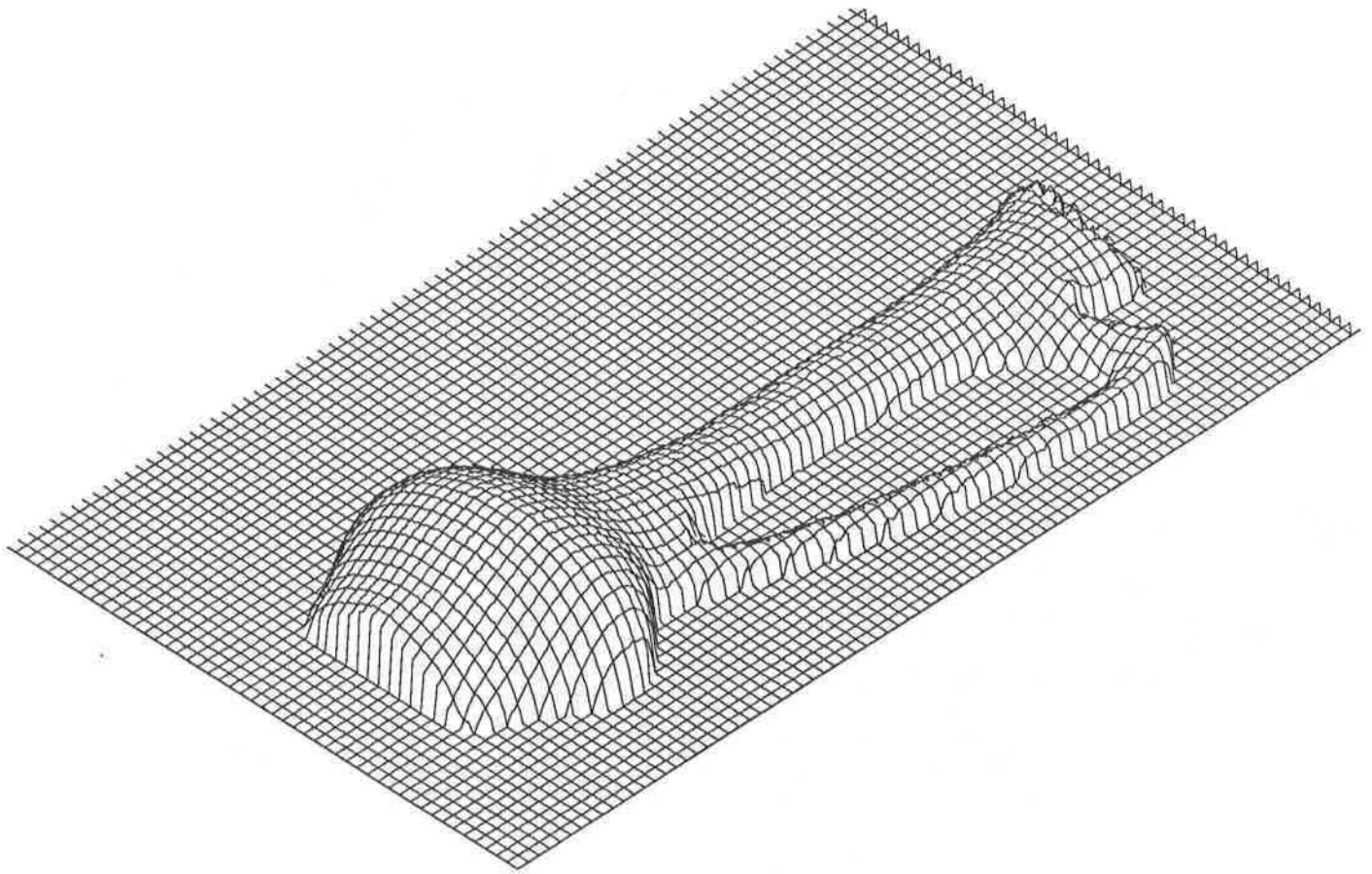


Figure 10: Result of **Experiment 3** – Coupled depth/slope model with prescribed boundary values being zero on the side boundaries and natural boundary conditions being imposed on the top and bottom boundaries.

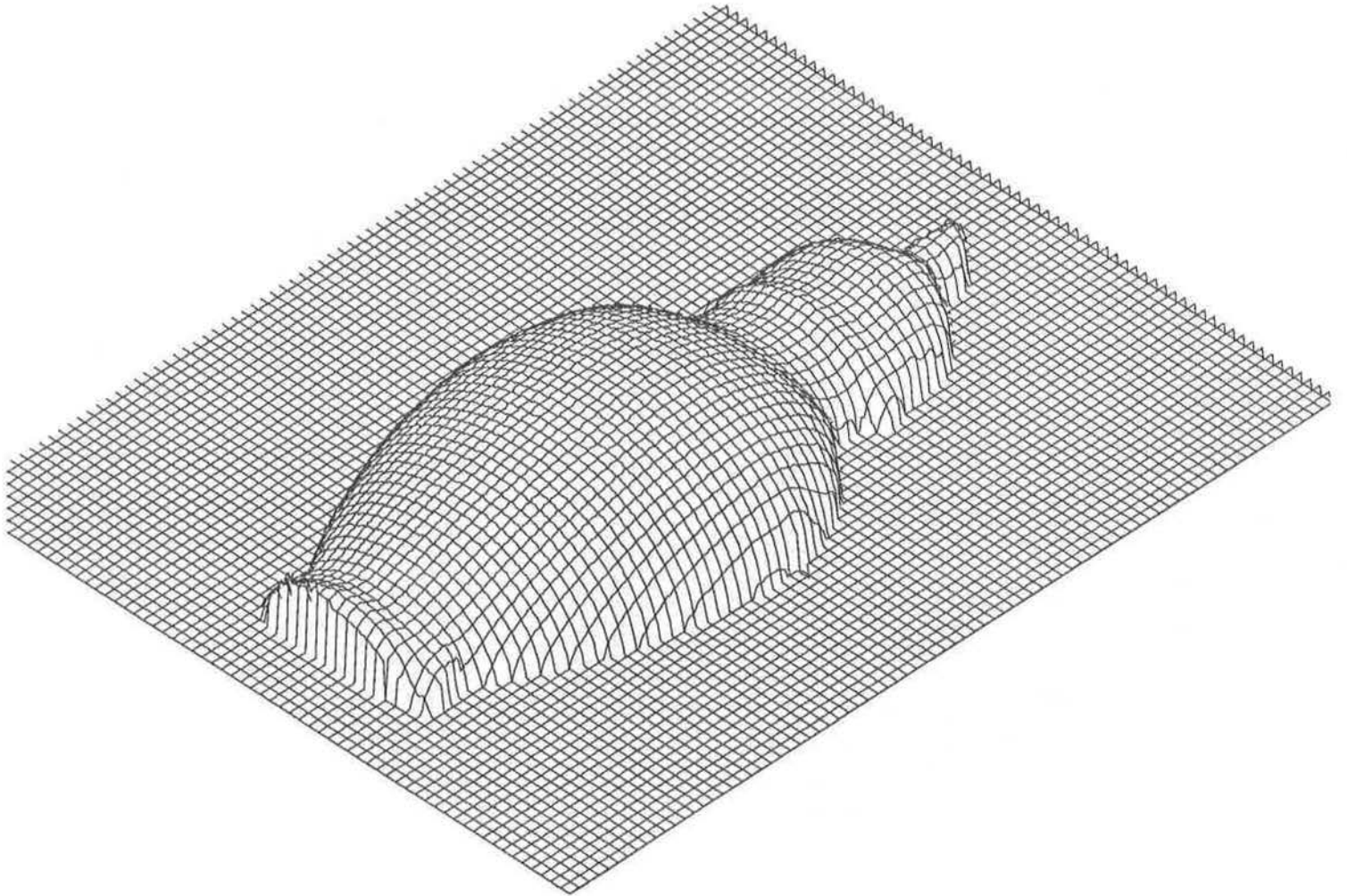


Figure 11: Result of **Experiment 3** – Coupled depth/slope model with prescribed boundary values being zero on the side boundaries and natural boundary conditions being imposed on the top and bottom boundaries.

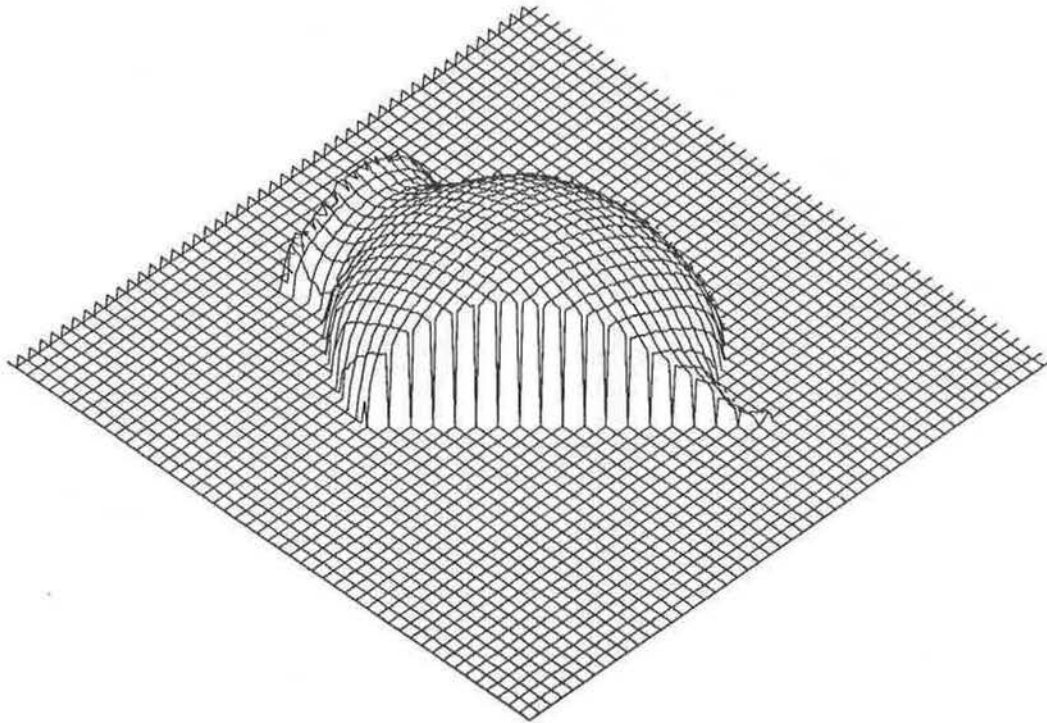


Figure 12: Result of **Experiment 4** – Coupled depth/slope model with prescribed boundary values being zero on the side boundaries and natural boundary conditions being imposed on the top and bottom boundaries. The new region is obtained by cutting the upper-right corner of the original region by slope 1.

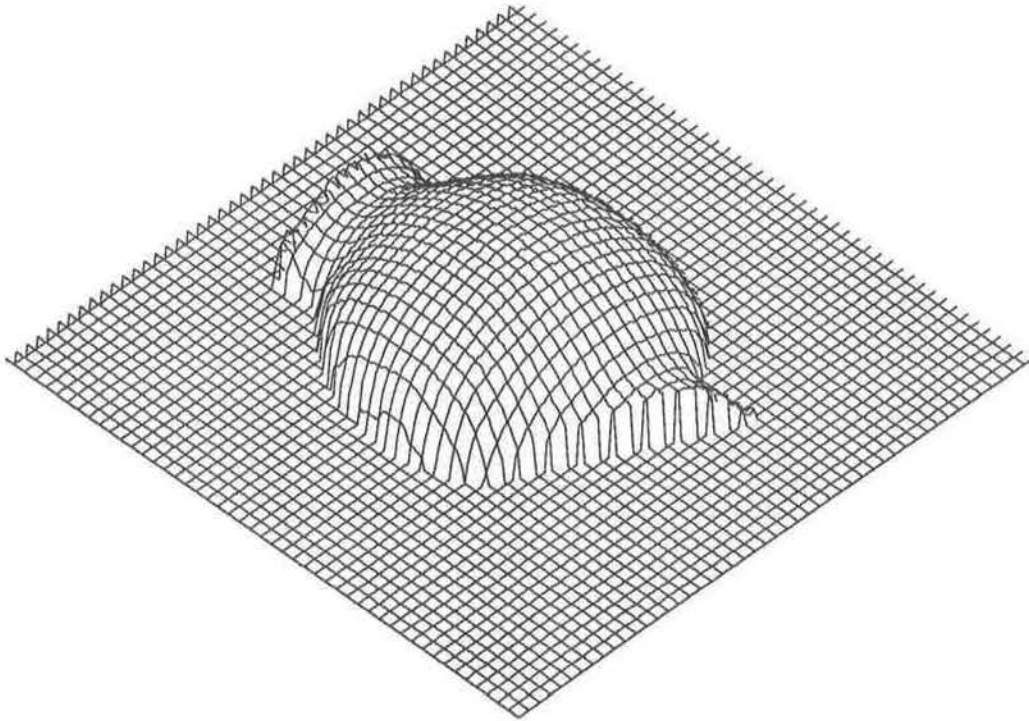


Figure 13: Result of **Experiment 4** – Coupled depth/slope model with prescribed boundary values being zero on the side boundaries and natural boundary conditions being imposed on the top and bottom boundaries. The new region is obtained by cutting the upper-right corner of the original region by slope $1/2$.

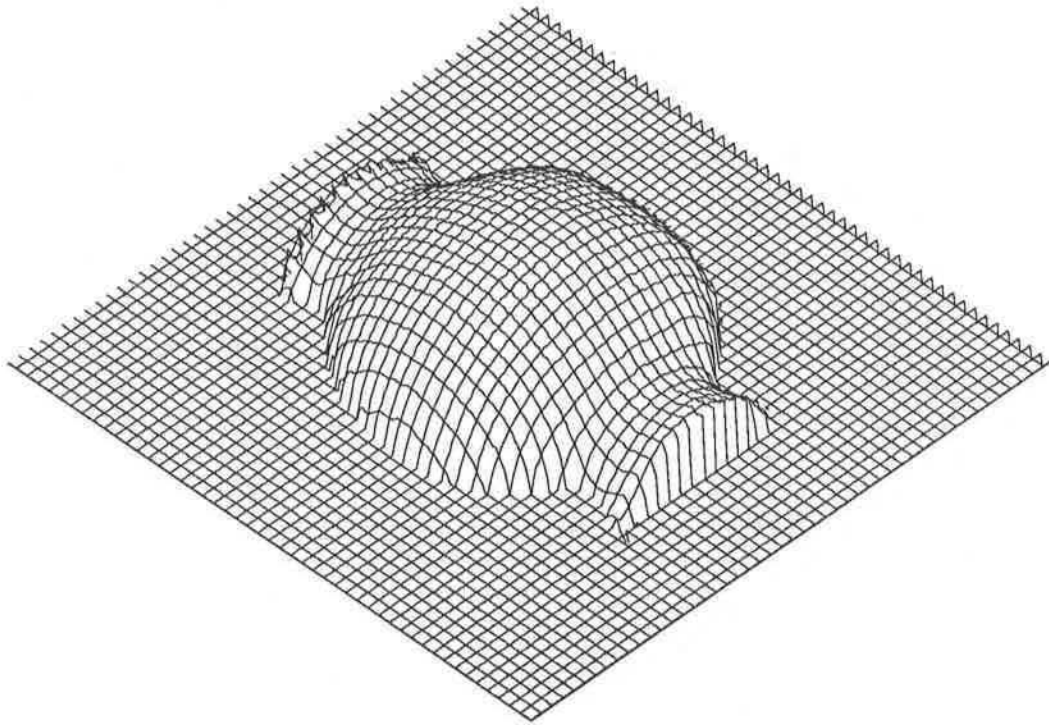


Figure 14: Result of **Experiment 4** – Coupled depth/slope model using transposed *s-array*, *p-array*, and *q-array* with natural boundary conditions being imposed on the straight side boundaries and the prescribed boundary values being zero on the curly top and bottom boundaries.

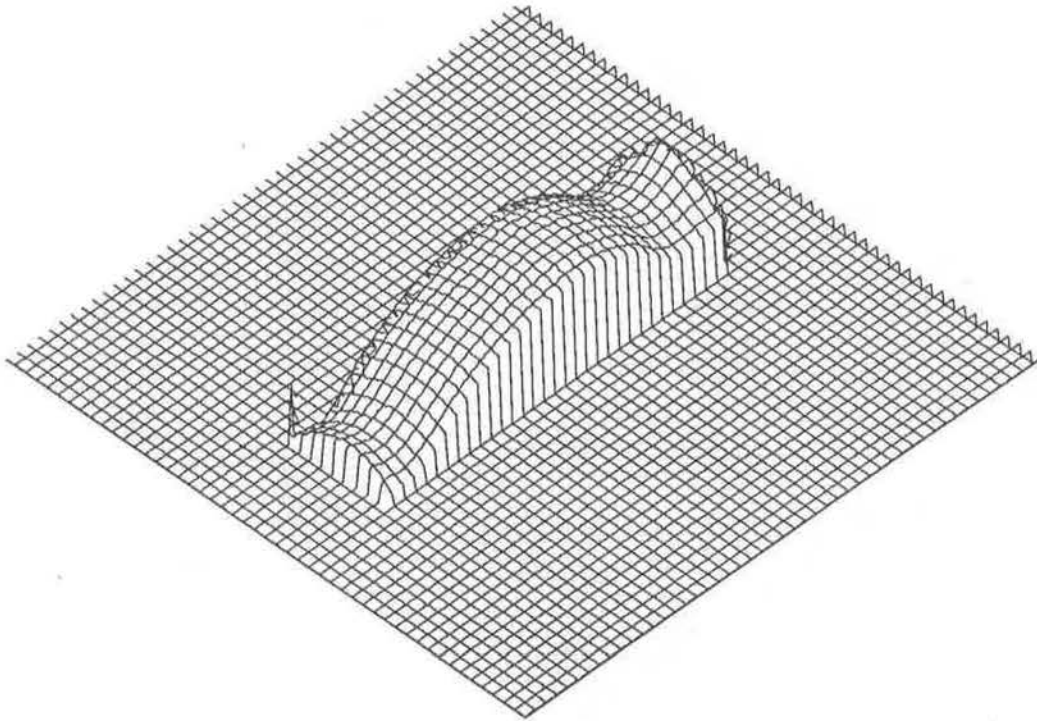


Figure 15: Result of **Experiment 5** – Coupled depth/slope model with natural boundary conditions being imposed on the whole boundary. The new region is obtained by cutting the original region vertically and throwing away the parts that are close to the side occluding boundary.

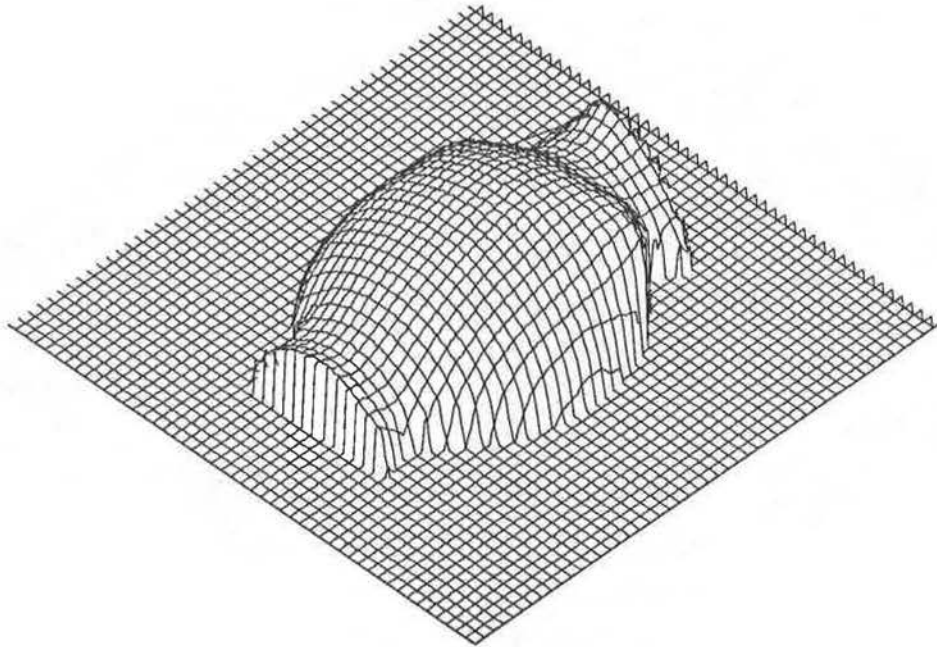


Figure 16: Result of **Experiment 6** – Coupled depth/slope model with occluding boundary points found by imposing natural boundary conditions on the whole boundary. The surface height is set to zero after the point is found to be on the occluding boundary.

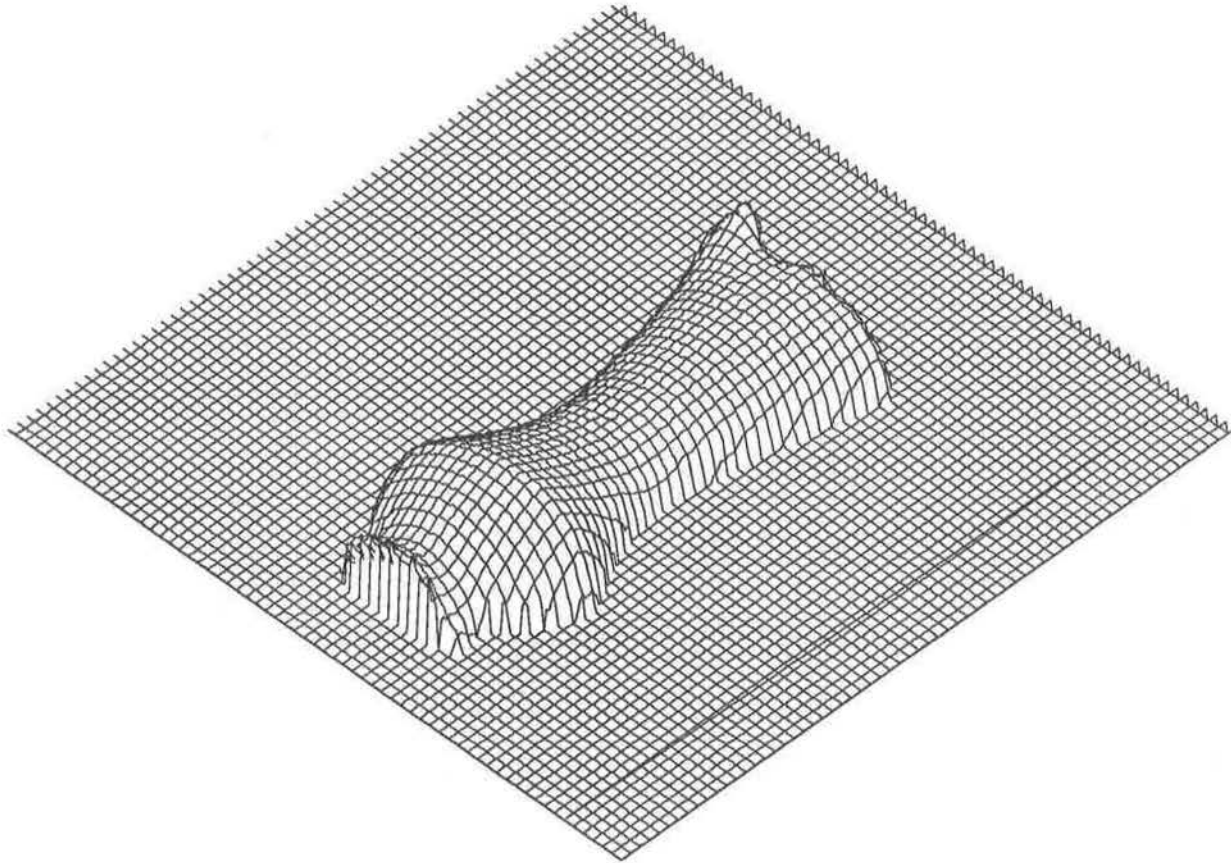


Figure 17: Result of **Experiment 6** – Coupled depth/slope model with occluding boundary points found by imposing natural boundary conditions on the whole boundary. The surface height is set to zero after the point is found to be on the occluding boundary.

References

- [1] R. Courant and D. Hilbert. *Methods of Mathematical Physics*, volume 1. Interscience Publishers, Inc., New York, 1953.
- [2] John G. Harris. The coupled depth/slope approach to surface reconstruction. Technical Report 908, Artificial Intelligence Laboratory, MIT, 1986.
- [3] Berthold K.P. Horn. Height and gradient from shading. A.I. Memo 1105, Artificial Intelligence Laboratory, MIT, 1989.
- [4] David G. Lowe. Organization of smooth image curves at multiple scales. *International Journal of Computer Vision*, 3:119 – 130, 1989.
- [5] D. Marr. Analysis of occluding contour. *Proc. R. Soc. Lond. B.*, 197:441 – 475, 1977.
- [6] Robert J. Woodham. Determining surface curvature with photometric stereo. In *Proc. 1989 IEEE International Conference on Robotics and Automation*, pages 36 – 42, Scottsdale, Arizona, 1989.